The role of hydrochlorofluorocarbon densifiers in the formation of clathrate hydrates in deep boreholes and subglacial environments

M. Mangir MURSHED,[1*] Sérgio H. FARIA,[1] Werner F. KUHS,[1] Sepp KIPFSTUHL,[2] Frank WILHELMS[2]

[1]*GZG, Abt. Kristallographie, Universität Göttingen, Goldschmidtstrasse 1, D-37077 Göttingen, Germany*
E-mail: murshed@uni-mainz.de
[2]*Alfred-Wegener-Institut für Polar- und Meeresforschung, Am Handelshafen 12, D-27570 Bremerhaven, Germany*

ABSTRACT. Clear evidence for the formation of mixed clathrate hydrates of air and hydrochlorofluorocarbon densifier (known as HCFC-141b, sometimes also called R-141b) is found by means of synchrotron X-ray diffraction and Raman spectroscopy on a sample recovered from the bottom of the EPICA Dronning Maud Land deep borehole in Antarctica. Subglacial water (SGW) appears to have reacted with the drilling liquid to build a large lump of clathrate hydrate. The hydrate growth may well have been accelerated by the stirring of the SGW–densifier mixture during drilling. Moreover, dissolved air in the SGW appears to have participated in the formation of mixed hydrates of air and HCFC-141b as evidenced by the concomitant appearance of Raman signals from both constituents. Our findings elucidate to some extent the meaning of earlier accounts of the formation of 'heavy chips' that may sink to the bottom of the borehole, possibly affecting or even impeding the drilling advance. These observations raise concerns with respect to the use of HCFC-141b densifiers in ice-core drilling liquids under warm ice conditions.

1. INTRODUCTION

Deep-drilling operations in polar ice sheets require the use of a fluid to fill the borehole with a bulk density that closely matches that of ice. This drilling fluid maintains the hydrostatic equilibrium in the borehole and thereby prevents its plastic collapse. Evidently, the drilling fluid must satisfy several criteria for density, viscosity, volatility, flammability, freezing point, frost resistance, safety, cost and environmental compliance (Talalay and Gundestrup, 2002). Besides, it must be chemically inert, i.e. it should not react in any way with the polar ice and its impurities, with the subglacial water (SGW) and its contents, with the chips produced by drilling or with any component of the drill itself. Exxsol™ D-series solvents (D-60, D-40, D-30) have been extensively employed as drilling fluids in the North Greenland Ice Core Project (NorthGRIP) and in the European Project for Ice Coring in Antarctica (EPICA). These fluids are de-aromatized, low-density liquids composed largely of organic solvents and blended with densifier additives such as hydrochlorofluorocarbon 141b (HCFC-141b, also abbreviated as R-141b). Interesting is the fact that HCFC-141b is known to form clathrate hydrates with structure type II (sII) at temperatures below 8.6°C under atmospheric pressure or any other pressure higher than 42 kPa (Brouwer and others, 1997; Ohmura and others, 1999). The behaviour at temperatures below 0°C is not known. However, from the established stability limits at temperatures above 0°C it can be expected that HCFC-141b hydrate is stable at temperatures below 0°C, at all pressures of interest here.

Part of the EPICA project included the extraction of a deep ice core from Dronning Maud Land, East Antarctica (EDML ice core; EPICA Community Members, 2006). This core was drilled at Kohnen station (75° S, 0° E; Drücker and others, 2002) during the period 2003–06, and D-40 blended with HCFC-141b was chosen as the drilling fluid. Liquid water was found at the bottom of the EDML borehole when drilling reached 2774.15 m depth. The presence of SGW indicates either ice-melting conditions at bedrock or the presence of a hydrological network beneath the EDML drilling site. Accordant with these conjectures is the fact that the lowest 2 m of the EDML ice core consist of ice that shows very low electrical conductivity and is essentially free of air hydrates.

Atmospheric gases (mainly N_2 and O_2) entrapped in air bubbles are known to gradually form sII air hydrates in deep polar ice at depths (>500 m) where the hydrostatic pressure is greater than the dissociation pressure of the hydrate phase (Miller, 1969; Shoji and Langway, 1982). On the other hand, SGW can be produced when the polar ice attains its melting point. This may happen beneath an ice sheet mainly because of three factors (Siegert, 2005). First, the hydrostatic pressure at the bottom of an ice sheet causes a sensible reduction in the ice-melting temperature (e.g. below 2800 m of ice this value is approximately –2.5°C). Second, the ice sheet insulates its base from the ultra-cold temperatures at the surface. Third, heat is supplied to the ice-sheet base by geothermal heating and is generated due to the flow of the ice sheet itself (frictional heat due to the deformation of ice and basal sliding). As a consequence, SGW may contain some amount of dissolved gases (Lipenkov and Istomin, 2001) coming from the air hydrates in the overlying ice. Therefore, care is required when choosing the drilling fluid and densifier, especially when SGW is concerned, because clathrate hydrates may form from the HCFC-141b densifier. The present study focuses on the formation of mixed clathrate hydrates of air and HCFC-141b in the SGW samples collected from the EDML borehole in 2006. Material found in the drill (Fig. 1) suggests that rapid blocking of ice-core drills in warm ice is linked to clathrate formation from water and the HCFC-141b densifier.

*Present address: Environmental Geochemistry Group, Institute of Geosciences, Johannes Gutenberg-Universität Mainz, Becher Weg 21, D-55099 Mainz, Germany.

https://doi.org/10.3189/172756407786857659 Published online by Cambridge University Press

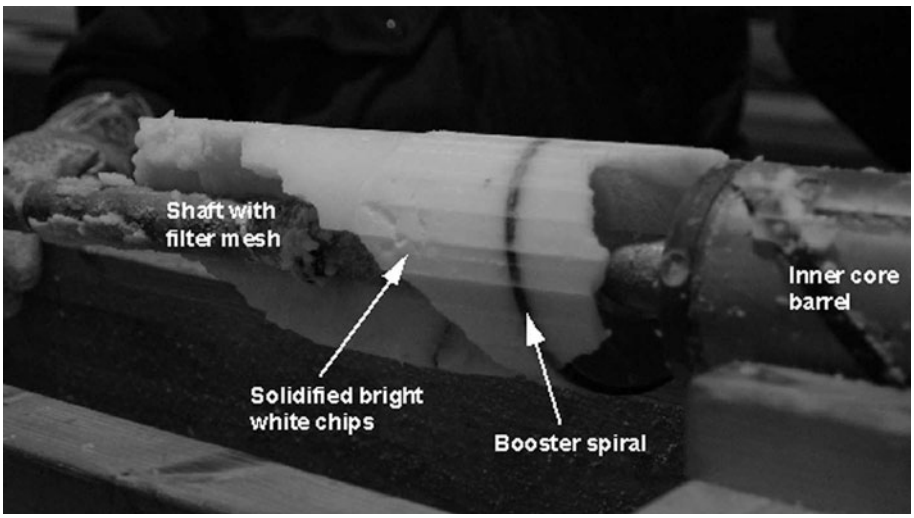

Fig. 1. Solidified bright white chips on the filter shaft from the chip chamber of the EDML drill during the cleaning procedure. The much brighter white appearance, compared to the common colour of the ice cuttings, suggests the presence of HCFC-141b clathrate hydrate, immediately after the drill arrived at the surface.

2. METHODS

A sample of SGW was collected from the bottom of the EDML borehole in January 2006. Since the drill had penetrated to the bottom from the colder surface and ice above (–40°C), the SGW froze in the drill almost immediately. On many occasions, rotation of the drill was halted due to freeze-up. Along with the frozen EDML SGW sample, a bright white hard material was observed. We show here that this material was HCFC-141b clathrate hydrate. We suggest it formed near the base of the borehole, where the pressures and temperatures are highest, and contributed to the drill freeze-up.

Since drilling, the sample has been stored at the Alfred Wegener Institute in Bremerhaven, Germany, for 6 months at –30°C and atmospheric pressure, then at Göttingen (and later Hamburg) to be investigated by X-ray diffraction (XRD) and Raman spectroscopy. When unpacking the samples for the analysis there was no indication of any change in the bright white appearance.

XRD measurements were performed using high-energy synchrotron radiation at the beamline BW5, HASYLAB, Hamburg. A comparative study of in-house X-ray and synchrotron diffraction for measuring natural hydrates has been published by Bohrmann and others (2007). The monochromatized and collimated photon beam ($\lambda =$ 0.1244 Å) was used as an incident X-ray beam that had a size of 1 mm^2 at the sample position. Such a small beam size ensures spatially resolved measurements for information on sample homogeneity. To study the homogeneity of the sample, we selected two different locations (10 mm apart) on the specimen. An image plate detector (mar345), placed 120 cm away from the sample, was used to register X-ray powder diffraction cones as Debye–Scherrer rings. Using the FIT2D program (Hammersley and others, 1996), these rings, recorded on a two-dimensional (2-D) detector, were integrated to the conventional 2-theta scans. Phase fractions of the samples were obtained from the XRD-data Rietveld refinements by using GSAS software (Larson and von Dreele, 2000). During refinements, general parameters such as the scale factor, background parameters, the zero point and the profile parameters were optimized. Notably, in the 2-D images, almost all the ice Ih rings in Debye–Scherrer patterns showed individual Bragg spots of very high intensity (>10 times higher) compared to any other point. In the FIT2D, facilities 'masking' tools (Bohrmann and others, 2007) have been used before integration, in order to obtain diffraction patterns that can be treated better in the GSAS Rietveld profile fitting, resulting in lower values of χ^2. Since the degree of masking (number and size of the high intense spots) is directly correlated to the peak intensity of a particular reflection of the respective constituents, some difference in the phase fractions (with/without masking) may be expected. For instance, using masking, the phase fractions differ by about 21% from the average value (without masking) in a sample from 100.89 m below the sea floor in the ODP Leg 204 sites (Bohrmann and others, 2007). The results of the quantitative phase analyses are given in Table 1.

Raman spectra were recorded on a Horiba Jobin Yvon HR800 ultraviolet micro-Raman spectrometer equipped with an air-cooled Ar laser working at 488 nm with a laser power of less than 20 mW. The laser beam was focused to a spot size of about 1–2 μm on the crushed/powder sample surface using an LWD Olympus ×50 objective lens. The confocal hole was closed to 200 μm. Spectra were collected in the range 200–4000 cm^{-1} with a resolution of about 0.8 cm^{-1} using a grating of 1200 grooves mm^{-1} and a Peltier-cooled charge-coupled device detector (Andor, 1024 × 256 pixels). The spectra were collected at –160°C using a Linkam (THMS 600) cooling stage to avoid any clathrate decomposition. A few grams of the samples were loaded, and three spectra were taken from three different grains (a, b, c) of the subglacial sample loaded each time.

3. RESULTS AND DISCUSSION

3.1. Structure refinement and XRD analysis

The starting parameters for sII hydrate refinements have been taken from Chazallon and Kuhs (2002) in the space group Fd-3m. At an early stage of the refinement, both the small (5^{12}) and the large ($5^{12}6^4$) cages were filled with nitrogen and oxygen, with 88% and 100% occupancy, respectively (Kuhs and others, 1997). After a few cycles of refinements,

https://doi.org/10.3189/172756407786857659 Published online by Cambridge University Press

the occupancy factor of the small cage had converged close to zero (±0.02) and of the large cage to ~3.7 times full occupancy, along with a high (unrealistic) thermal parameter. These results indicate that the small cages are almost vacant and the large cages are filled with larger molecules, i.e. with a molecular weight (MWt) approximately 3.7 times more than that of diatomic nitrogen or oxygen gas. In contrast, in a separate trial, taking CH_3CCl_2F (MWt = 116.95) as the large cage filler, the population parameter converged close to full occupancy (which was subsequently fixed in each final run to be exactly one molecule per cage), also yielding lower R-factors. At first approximation, this suggests that the observed sII hydrates are formed from a larger molecule such as the HCFC-141b densifier.

The synchrotron XRD-data Rietveld analysis (Fig. 2) provides access to the phase fractions of the constituents present in the sample as summarized in Table 1. Ice Ih is frequently found in the form of large crystallites impairing an isotropic orientational distribution, a prerequisite for standard Rietveld refinements. Therefore, we decided to mask the corresponding very strong diffraction spots of the powder image as described in Bohrmann and others (2007). The masking delivers too low values for the ice Ih phase fractions, but provides better estimates for the structural parameters of the hydrate phase. Consequently, the variations in the phase fractions could be due to local variation (on mm scale), sampling (crushed or millimetre-sized lumps) and/or pre-treatment (masking) of the XRD data before refinement. It is, however, unlikely that the local variations in ice Ih content are solely due to the masking technique, as the scatter between different samples is similar with and without masking. As a result, we obtain an averaged cell parameter of about 17.210(5) Å, measured at –203°C; this is larger than the value found in the literature for air hydrate (17.14 Å at –146°C; Takeya and others, 2000) and slightly smaller than halogen hydrocarbon clathrate hydrates (17.234(3) Å at about –183°C; Brouwer and others, 1997). Hence, we are inclined to ascribe the hydrate investigated to higher hydrocarbons and not to air clathration, confirming the result of the occupancy analysis presented above. Measurements at different locations (10 mm apart) on the same sample indeed do not show any substantial difference in cell parameter. Nevertheless our X-ray study leaves open

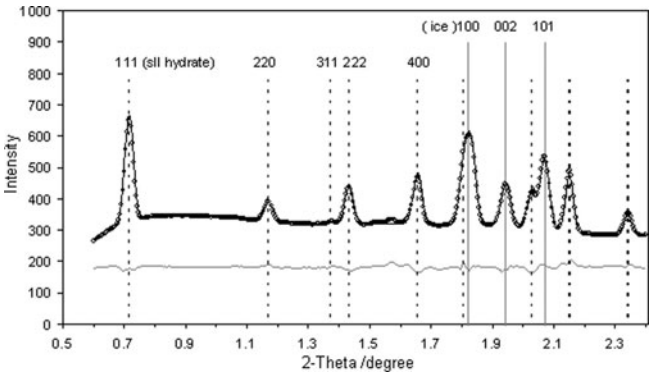

Fig. 2. Rietveld plot of the synchrotron XRD data of the crushed subglacial sample with observed pattern (open circles), calculated pattern (solid black curve), and difference between observed and calculated (solid grey curve below). Vertical dashed and solid lines indicate possible positions of Bragg reflections of hydrate sII and ice Ih, respectively.

the question of whether the investigated samples include some air molecules in the cages. Moreover, the refined phase fractions indicate some heterogeneity of the ice/clathrate-hydrate ratio within the sample on the millimetre scale (Table 1); within this mix of phases, neither can the existence of isolated air hydrate crystals be excluded. It should also be noted that at least one other phase occurs in the SGW sample, indicated by very weak peaks which could not be indexed.

We are not aware of any report of a high-pressure phase diagram of an HCFC-141b/water system (i.e. pressures comparable to those in the lower part of the EDML borehole). It is reasonable to assume, however, that HCFC-141b sII hydrate forms in the HCFC-141b/SGW liquid–liquid system (Ohmura and others, 1999; Kato and others, 2000; Sakaguchi and others, 2003) irrespective of the formation mechanism, i.e. hydrate formation at the hydrate/water phase boundaries or in the bulk of water phase (Sloan and Koh, 2007). Indeed, the pressure and temperature conditions throughout the borehole are far above the equilibrium/extrapolated-equilibrium line (Brouwer and others, 1997; Ohmura and others, 1999).

Table 1. Results of the synchrotron XRD-data Rietveld refinements

Sample	Exp.	Masking*	Cell (sII) Å	Ice Ih α	sII α	χ^2	R_{Wp}
SGWP	1	no	17.210	75.7(8)	24.3(22)	29.9	26.0
SGWP	1	yes	17.210(6)	38.3(4)	61.7(3)	0.3	3.0
SGWP	2	no	17.225	59.5(20)	40.5(30)	34.8	29.2
SGWP	2	yes	17.225(3)	46.3(3)	53.7(4)	0.4	3.4
SGWL	3	no	17.200	72.8(20)	27.2(42)	201.5	56.7
SGWL	3	yes	17.200(4)	9.3(5)	90.7(1)	0.2	2.7
SGWL	4	no	17.206	74.4(17)	25.6(42)	122.7	49.0
SGWL	4	yes	17.206(6)	15.8(7)	84.2(2)	0.3	3.2

Notes: Phase fractions (α) of hexagonal ice (Ih) and clathrate hydrate (sII) are given as percentages. SGWP = crushed/powder; SGWL = 3–4 mm sized lumps. Experiments with identical number denote measurements at different locations (10 mm apart) of the same sample. The *a* and *c* parameters of ice Ih are refined and fixed at 4.503 and 7.327, respectively, in the final run for all the refinements. The more reliable results for the lattice constants obtained in the masked refinements were used and kept fixed in the treatment of the unmasked datasets. R_{Wp}: residual weight pattern.
*Details are available in Bohrmann and others (2007).

https://doi.org/10.3189/172756407786857659 Published online by Cambridge University Press

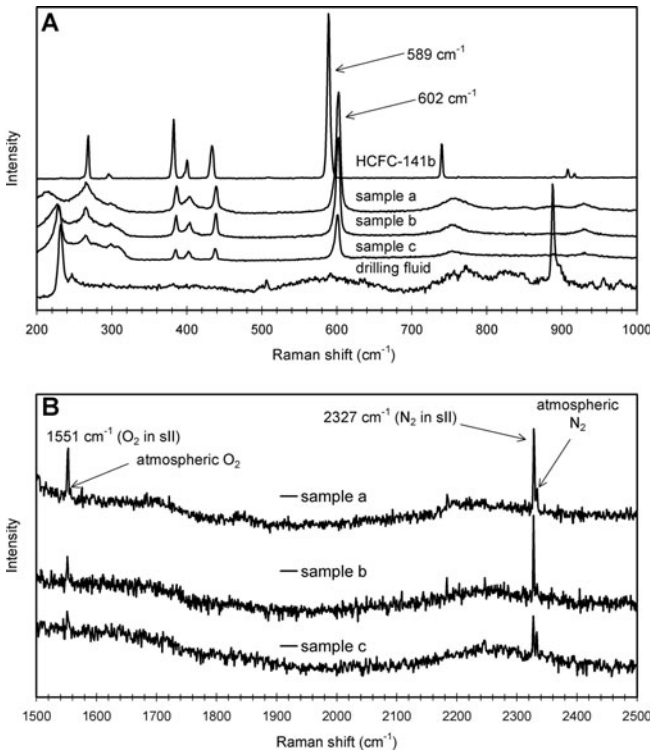

Fig. 3. The Raman spectra in the range 200–4000 cm^{-1} of the subglacial samples (samples a, b, c) and the solidified drilling fluid (D-40 + HCFC-141b) measured at –160°C, along with the reference liquid HCFC-141b at room temperature, are split into two ranges of interest. a, b, c refer to three subglacial grains loaded as different sampling for Raman measurement. (a) The Raman spectra in the region 200–1000 cm^{-1} depict mainly the shift of the carbon–halogen stretch mode of liquid HCFC-141b to higher wavenumber on HCFC-141b hydrate formation. (b) The spectra of samples a, b and c in the range 1500–2500 cm^{-1} show the stretching modes of nitrogen and oxygen, where the intensity (*y* axis) has been rescaled to enhance the view of the weak bands of oxygen and nitrogen enclathrated in the hydrate sII structure.

3.2. Raman investigation

Although a number of works have been published on HCFC-141b hydrates (Ohmura and others, 1999; Kato and others, 2000; Liang and others, 2001; Sakaguchi and others, 2003), Raman investigations of these hydrates are scarce. Recently, Greathouse and others (2007) reported HCFC-141b hydrates, and the dynamics of guest HCFC-141b molecules within water cages by ab initio calculations, molecular dynamics simulations and Raman spectroscopy. The frequency of a carbon–halogen stretch mode (~585 cm^{-1}) undergoes a shift to higher wavenumber in the hydrate phase, which is in agreement among the vibration frequency data obtained from two computational methods, and Raman experiments at 0°C. The Raman carbon–halogen stretch mode of liquid HCFC-141b (586.03 cm^{-1}) shifted ~ 7.5 cm^{-1} to higher wavenumber (593.44 cm^{-1}) on HCFC-141b hydrate formation. In contrast, we observed the corresponding peak of the reference HCFC-141b liquid at 589 cm^{-1} at room temperature, which shifted to 602 cm^{-1} for the subglacial HCFC-141b hydrate measured at –160°C (Fig. 3a). Notably, the temperature-induced shift of the HCFC-141b liquid peak at 586 cm^{-1} is less than 0.3 cm^{-1} between –78°C and 0°C (Bradshaw and others, 2006). Therefore, the frequency value of this particular carbon–halogen peak in the subglacial samples (samples a, b, c; Fig. 3a) clearly indicates the changes of vibration frequencies of the HCFC-141b molecule in the water cage due to host–guest interactions. Other bending modes associated with halogen and carbon atoms occur at lower frequencies (<600 cm^{-1}), which are close to the reported values (Greathouse and others, 2007). However, the corresponding peaks are not clearly resolved in the solidified drilling fluid (D-40 with densifier), probably because of the low concentration of the densifier. From the initial concentration of less than 23% by volume, the HCFC-141b densifier is depleted with the ice cuttings in the hole and is largely evaporated while collecting drilling liquid during the core recovery at the surface. Thus, only small amounts of densifier are expected in the recovered drilling liquid sample.

In contrast to the intensity of the peaks of HCFC-141b hydrates, two weak bands (Fig. 3b) at 2327 cm^{-1} and 1551 cm^{-1} have been observed in the same spectrum. The former band is attributed to nitrogen and the latter to oxygen in the clathrate structure. This is in good agreement with the reported values for synthetic air hydrates (Chazallon and others, 1998) and is comparable with values for natural samples collected from deep ice cores (Nakahara and others, 1988; Pauer and others, 1995). A shoulder at 2333 cm^{-1} can be assigned to the vibron modes of atmospheric nitrogen (2331 cm^{-1}; Herzberg, 1950). However, the corresponding modes of atmospheric oxygen at 1556 cm^{-1} (Herzberg, 1950; Bier and Jodl, 1984) could not be resolved from the noise.

The storage conditions at the drilling site and, later, in Bremerhaven were not ideal for preserving air hydrates, and some decomposition may have occurred (while HCFC-141b hydrates are expected to be perfectly stable under the recovery, transport and storage conditions). At first glance, the pressure and temperature conditions in the lower part of the borehole were quite favorable to form N_2, O_2 or air hydrate (Van Cleeff and Diepen, 1965; Tse and others, 1986; Kuhs and others, 1997, 2000). However, the formation kinetics of air hydrate are expected to be much slower than those of HCFC-141b hydrate, due to the markedly higher equilibrium pressure (and correspondingly lower driving force) of the former. Pure air hydrate will only nucleate easily at a water–air interface, as the activity of nitrogen/oxygen in the dissolved state in water is likely to be too low for nucleation. Pre-existing air hydrates liberated from the ice matrix upon melting of the latter will eventually decompose as the concentration/activity of air at the interface is reduced by the high diffusion coefficients of air in water. During the short extraction time of the SGW sample of about 1 hour (passing through a lower-temperature regime) air hydrate formation is not expected to an appreciable extent. Rather, it is reasonable to suppose that the dissolved air in the SGW participated in the growth of *mixed hydrates* (of air and HCFC-141b) at the bottom of the borehole.

3.3. Relation to former studies

Gundestrup and others (2002) performed an experiment at –15°C and atmospheric pressure by blending ice chips with Exxon D-60 mixed with HCFC-141b densifier. After a week of contact, the ice chips separated into three fractions: larger ice crystals floated on the liquid, smaller ice crystals were observed suspended in the liquid and some of them sedimented at the bottom. However, at similar pressure–temperature conditions, an experiment employing HCFC-123 as densifier showed that all ice chips floated on the

https://doi.org/10.3189/172756407786857659 Published online by Cambridge University Press

liquid. Talalay and Gundestrup (1999) and Gundestrup and others (2002) argued that the HCFC-141b densifier influenced the ice in such a way that the ice chips became heavier. There is no allusion in these reports to clathrate hydrate formation, but since the pressure–temperature conditions were well inside the stability field (Brouwer and others, 1997), we cannot rule out HCFC-141b hydrate formation.

During the drilling at NorthGRIP, Greenland, and at Dome C, Antarctica, Exxon D-60 and Exxon D-30 respectively were used (Talalay and Gundestrup, 1999). In both cases, HCFC-141b was used as densifier, and electromechanical drills of the same type were stuck at depths of 1371 m (1997, NorthGRIP) and 786 m (1998, Dome C). Talalay and Gundestrup (1999) and Gundestrup and others (2002) argued that ice chips might have slowly formed sediment which probably was one of the causes of the drills sticking. We assume that in both cases HCFC-141b hydrate might form. Clathrate growth kinetics are best established for temperatures near 0°C, yet it has been found that also at temperatures as low as –50°C appreciable clathrate growth can take place (Genov and others, 2004). Hondoh and others (1990) calculated the density of natural air hydrate (Greenland Dye-3 deep ice core) as 980 kg m^{-3}, i.e. higher than ice (920 kg m^{-3}) at the investigated temperature (–30°C). The density of HCFC-141b hydrate is expected to be even higher: from the averaged lattice constant at –203°C we obtain ~1102 kg m^{-3}. Assuming thermal expansivity similar to the TFP + CH_4 hydrate case (Huo, 2002; Sloan and Koh, 2007), the density is calculated as ~1064 kg m^{-3} at –30°C, a temperature relevant to deep-drilling operations in polar ice. It is therefore expected that what those authors (Talalay and Gundestrup, 1999; Gundestrup and others, 2002) anticipated as ice chips might also have included HCFC-141b clathrate hydrate, which sank and accumulated in the lower part of the borehole. Additionally, it is not surprising that some HCFC-141b hydrate may form at the expense of the thawed ice (or even liquid water) produced from the friction between the drill and the ice core (Árnason and others, 1974; Azuma and others, 2007). Indeed, it has frequently been observed that hydrate formation is particularly rapid close to the ice melting point (Stern and others, 1996), suggesting that a rather complete formation of HCFC-141b hydrate may take place on a timescale of a few minutes to hours near 0°C, in particular when stirring is also active.

4. CONCLUSION

X-ray and Raman investigations of a frozen SGW sample from the EDML deep borehole in Antarctica revealed that at least a substantial part of the sample consists of sII clathrate hydrates. The drilling-fluid densifier HCFC-141b has been identified as one of the main sII hydrate formers, supposed to react with SGW in the borehole during drilling.

As the densifier forms hydrates with the SGW, it raises several concerns. Among them, the borehole may become blocked at the SGW surface by forming a solid lump of hydrate at the interface with the drilling fluid. HCFC-141b has also been claimed to 'bond', to a limited extent, to ice chips within the borehole, thereby increasing their density (Talalay and Gundestrup, 2002). Over a long period of time, such chips may sink to the bottom of the borehole to form slush. This may raise a problem even in normal drilling conditions, because the accumulation of chips at the bottom of the borehole makes drill penetration difficult. Moreover, these dense chips may contribute to the sticking of the drill when the driller ignores the possibility of a slushy bottom following a long period of pause such as the long overwinter of inactivity. Therefore, care must be taken in choosing the drilling fluid, especially when the SGW is concerned. Indeed, the subglacial environment is nowadays recognized as very vulnerable to contamination and HCFC-141b could be dispersed through hydrate formation. However, whether a HCFC-141b hydrate formation does accelerate the contamination by some drifting of small hydrate particles or whether the hydrate acts as a temporary seal retarding further contamination must remain undecided at present. The observed formation of HCFC-141b clathrate hydrate explains the abrupt termination of a major fraction of drill runs in the warm ice, where the drill suddenly blocks completely and a bright white material is found between ice core and core barrel or in the chip-transport system of the drill. Thus, prospective new drilling liquids should also be screened for their ability to form clathrate hydrate together with the ice or free water.

ACKNOWLEDGEMENTS

We thank B. Schmidt for help with the Raman measurements and H. Klein for help with the synchrotron data collection. We thank Hamburger Synchrotronstrahlungslabor (HASYLAB) at Deutsches Elektronen Synchrotron (DESY) for providing beam time and support. This work was funded in part by the German Ministry of Education and Research (BMBF) and the German Research Foundation (DFG) in the programme GEOTECHNOLOGIEN, of which this is publication No. GEOTECH-293. This work is a contribution to the European Project for Ice Coring in Antarctica (EPICA publication No. 209), a joint European Science Foundation/European Commission scientific programme, funded by the European Union (EPICA-MIS) and by national contributions from Belgium, Denmark, France, Germany, Italy, the Netherlands, Norway, Sweden, Switzerland and the United Kingdom. The main logistic support was provided by Institut Polaire Français–Emile Victor (IPEV) and Programma Nazionale di Ricerche in Antartide (PNRA) (at Dome C) and the Alfred Wegener Institute (at Dronning Maud Land).

REFERENCES

Árnason, B., H. Björnsson and P. Theodórsson. 1974. Mechanical drill for deep coring in temperate ice. *J. Glaciol.*, **13**(67), 133–139.

Azuma, N., I. Tanabe and H. Motoyama. 2007. Heat generated by cutting ice in deep ice-core drilling. *Ann. Glaciol.*, **47**, 61–67.

Bier, K.D. and H.J. Jodl. 1984. Influence of temperature on elementary excitations in solid oxygen by Raman studies. *J. Chem. Phys.*, **81**(3), 1192–1197.

Bohrmann, G. *and 6 others*. 2007. Appearance and preservation of natural gas hydrate from Hydrate Ridge sampled during ODP Leg 204 drilling. *Mar. Geol.*, **244**(1–4), 1–14.

Bradshaw, R., W. Clift, D. Dedrick, E. Majzoub and B. Simmons. 2006. Clathrate hydrates for production of potable water. *Mater. Res. Soc. Symp. Proc.*, **930**, 14–19.

Brouwer, D.H., E.B. Brouwer, G. Maclaurin, M. Lee, D. Parks and J.A. Ripmeester. 1997. Some new halogen-containing hydrate-formers for structure I and II clathrate hydrates. *Supramol. Chem.*, **8**(4), 361–367.

Chazallon, B. and W.F. Kuhs. 2002. In situ structural properties of N_2-, O_2-, and air-clathrates by neutron diffraction. *J. Chem. Phys.*, **117**(1), 308–320.

https://doi.org/10.3189/172756407786857659 Published online by Cambridge University Press

Chazallon, B., B. Champagnon, G. Panzcer, F. Pauer, A. Klapproth and W.F. Kuhs. 1998. Micro-Raman analysis of synthetic air clathrate hydrate. *Eur. J. Mineral.,* **10**(6), 1–10.

Drücker, C., F. Wilhelms, H. Oerter, A. Frenzel, H. Gernandt and H. Miller. 2002. Design, transport, construction, and operation of the summer base Kohnen for ice-core drilling in Dronning Maud Land, Antarctica. *Mem. Natl. Inst. Polar Res.,* **56**, Special Issue, 302–312.

EPICA Community Members. 2006. One-to-one coupling of glacial climate variability in Greenland and Antarctica. *Nature,* **444**(7116), 195–198.

Genov, G., W.F. Kuhs, D.K. Staykova, E. Goreshnik and A.N. Salamatin. 2004. Experimental studies on the formation of porous gas hydrates. *Am. Mineral.,* **89**(8–9), 1228–1239.

Greathouse, J.A., R.T. Cygan, R.W. Bradshaw, E.H. Majzoub and B.A. Simmons. 2007. Computational and spectroscopic studies of dichlorofluoroethane hydrate structure and stability. *J. Phys. Chem.,* **11**(45), 16,787–16,795.

Gundestrup, N.S., S.J. Johnsen, S.B. Hansen, H. Shoji, P. Talalay and F. Wilhelms. 2002. Sticking deep ice core drills. Why and how to recover. *Mem. Natl. Inst. Polar Res.,* **56**, Special Issue, 181–195.

Hammersley, A.P., S.O. Svensson, M. Hanfland, A.N. Fitch and D. Hausermann. 1996. Two-dimensional detector software: from real detector to idealised image or two-theta scan. *High Pres. Res.,* **14**(4–6), 235–248.

Herzberg, G. 1950. *Molecular spectra and molecular structure. I. Spectra of diatomic molecules*. Ottawa, Ont., National Research Council of Canada.

Hondoh, T., H. Anzai, A. Goto, S. Mae, A. Higashi and C.C. Langway, Jr. 1990. The crystallographic structure of the natural air-hydrate in Greenland Dye-3 deep ice core. *J. Incl. Phenom. Macrocyc. Chem.,* **8**(1–2), 17–24.

Huo, Z. 2002. Hydrate phase equilibria measurements by X-ray diffraction and Raman spectroscopy. (PhD thesis, Colorado School of Mines.)

Kato, M., T. Iida and Y.H. Mori. 2000. Drop formation behaviour of a hydrate-forming liquid in a water stream. *J. Fluid Mech.*, **414**, 367–378.

Kuhs, W.F., B. Chazallon, G. Radaelli and F. Pauer. 1997. Cage occupancy and compressibility of deuterated N_2-clathrate hydrate by neutron diffraction. *J. Incl. Phenom. Macrocyc. Chem.,* **29**(1), 65–77.

Kuhs, W.F., A. Klapproth and B. Chazallon. 2000. Chemical physics of air clathrate hydrates. *In* Hondoh, T., *ed. Physics of ice core records.* Sapporo, Hokkaido University Press, 373–392.

Larson, A.C. and R.B. von Dreele. 2000. General structure analysis system (GSAS). *Los Alamos National Laboratory Report* LAUR 86-748.

Liang, D., K. Guo, R. Wang and S. Fan. 2001. Hydrate equilibrium data of 1,1,1,2-tetrafluoroethane (HFC-134a), 1,1-dichloro-1-fluoroethane (HCFC-141b) and 1,1-difluoroethane (HFC-152a). *Fluid Phase Equilib.*, **187–188**, 61–70.

Lipenkov, V.Y. and V.A. Istomin. 2001. On the stability of air clathrate-hydrate crystals in the subglacial Lake Vostok, Antarctica. *Mater. Glyatsiol. Issled.* 91, 129–137.

Miller, S.L. 1969. Clathrate hydrates of air in Antarctic ice. *Science,* **165**(3892), 489–490.

Nakahara, J., Y. Shigesato, A. Higashi, T. Hondoh and C.C. Langway, Jr. 1988. Raman spectra of natural clathrates in deep ice cores. *Philos. Mag. B,* **57**(3), 421–430.

Ohmura, R., T. Shigetomi and Y. H. Mori. 1999. Formation, growth and dissociation of clathrate hydrate crystals in liquid water in contact with a hydrophobic hydrate-forming liquid. *J. Cryst. Growth,* **196**(1), 164–173.

Pauer, F., J. Kipfstuhl and W.F. Kuhs. 1995. Raman spectroscopic study on the nitrogen/oxygen ratio in natural ice clathrates in the GRIP ice core. *Geophys. Res. Lett.,* **22**(8), 969–971.

Sakaguchi, H., R. Ohmura and Y.H. Mori. 2003. Effects of kinetic inhibitors on the formation and growth of hydrate crystals at a liquid–liquid interface. *J. Cryst. Growth,* **247**(3–4), 631–641.

Shoji, H. and C.C. Langway, Jr. 1982. Air hydrate inclusions in fresh ice core. *Nature,* **298**(5874), 548–550.

Siegert, M.J. 2005. Lakes beneath the ice sheet: the occurrence, analysis, and future exploration of Lake Vostok and other Antarctic subglacial lakes. *Annu. Rev. Earth Planet. Sci.,* **33**, 215–245.

Sloan, E.D., Jr and C. Koh. 2007. *Clathrate hydrates of natural gases. Third edition.* Boca Raton, FL, CRC Press.

Stern, L.A., S.H. Kirby and W.B. Durham. 1996. Peculiarities of methane clathrate hydrate formation and solid-state deformation, including possible superheating of water ice. *Science,* **273**(5283), 1843–1848.

Takeya, S., H. Nagaya, T. Matsuyama, T. Hondoh and V.Y. Lipenkov. 2000. Lattice constants and thermal expansion coefficient of air clathrate hydrate in deep ice cores from Vostok, Antarctica. *J. Phys. Chem. B,* **104**(4), 668–670.

Talalay, P.G. and N.S. Gundestrup. 1999. *Hole fluids for deep ice core drilling: a review.* Copenhagen, University of Copenhagen.

Talalay, P.G. and N.S. Gundestrup. 2002. Hole fluids for deep ice core drilling. *Mem. Natl. Inst. Polar Res.,* **56**, Special Issue, 148–170.

Tse, J.S., Y.P. Handa, C.I. Ratcliffe and B.M. Powell. 1986. Structure of oxygen clathrate hydrate by neutron powder diffraction. *J. Incl. Phenom.,* **4**(3), 235–240.

Van Cleeff, A. and G.A.M. Diepen. 1965. Gas hydrates of nitrogen and oxygen II. *Recl Trav. Chim.,* **84**, 1085–1093.

https://doi.org/10.3189/172756407786857659 Published online by Cambridge University Press